European Polymer Journal 98 (2018) 72–82

Contents lists available at ScienceDirect

European Polymer Journal

journal homepage: www.elsevier.com/locate/europolj

Analysis of microstructure and mechanical performance of polymeric cellular structures designed using stereolithography

Sofiane Guessasma[a,b,*], Liu Tao[b], Sofiane Belhabib[c], Jihong Zhu[b], Weihong Zhang[b], Hedi Nouri[d]

[a] INRA, UR1268 Biopolymères Interactions Assemblages, F-44300 Nantes, France
[b] Laboratory of Engineering Simulation & Aerospace Computing-ESAC, Northwestern Polytechnical University, 710072 XiAn, Shaanxi, China
[c] LUNAM University of Nantes Angers Le Mans, CNRS, GEPEA, UMR 6144, IUT de Nantes, 2 avenue du Professeur Jean Rouxel, 44475 Carquefou Cédex, France
[d] Department of Polymers and Composites Technology & Mechanical Engineering, Mines Douai, 941 rue Charles Bourseul, CS 10838, F-59508 Douai, France

ARTICLE INFO

Keywords:
Stereolithography
Finite element computation
Compressive response
Cellular polymer
X-ray micro-tomography
Damage – densification model

ABSTRACT

The aim of this work is to deliver a precise statement about the mechanical effect of microstructural defects induced by stereolithography. Design of cellular structures based on a photosensitive resin with varied porosity content is performed up to 60%. The compressive behaviour of these structures is captured and microstructural defects are analysed using X-ray micro-tomography. Finite element computation is considered to predict the compressive behaviour of both 3D microstructures and CAD (Computer-Aided Design) models up to the densification stage. X-ray micro-tomography analyses reveals that two main defects are generated by the process, namely residual support material and excess of resin trapped inside the porous network. Significance of the defects is proved to be related to the design of cellular structures with porosity levels in the range 10–30%. In addition, both experimental and numerical results show no evidence of anisotropic effect related to additive layering of resin. Finally, the suggested damage – densification constitutive law captures the main characteristics of the compressive response of studied cellular structures.

1. Introduction

Cellular solids, which are media composed of solid and gaseous phases, have particular performance that can be modulated in a wide range by manipulating their airy nature [1]. Indeed, cellular solids are widely used in applications requiring lightweight performance [2], thermal insulation [3], energy and noise absorption [4], filtering (Yadroitsev et al., 2009), and substitutes for tissue engineering [5]. These applications impose stringent restrictions on the cellular morphology. Conventional manufacturing methods like foaming and powder metallurgy experience difficulties to control the internal microstructural cellular structures, causing the low repeatability of desired morphology and deviation from targeted properties. Therefore, the obtained properties are highly sensitive to scale change because of the differences that appear between local and global measurements such as for density, feature size and shape. Additive manufacturing (AM) allows the fabrication of parts exhibiting complex geometries. On top of being reproducible, these AM parts share the key advantage of offering predictable and pre-determined unit cells even with interconnected porous structures [6].

Some of the most popular AM systems include stereolithography (SL), laser sintering (LS), fused deposition modelling (FDM) and laminated object manufacturing (LOM), which use liquid, filament/paste, powder and solid sheet material, respectively [7]. Stereolithography (SL) is one of these AM techniques, which exhibit high fabrication accuracy. The increasing number of available materials that are now used as a feedstock material for stereolithography allows stereolithography to fairly compete with traditional process routes for polymer manufacturing. Stereolithography has received remarkable success in applications of manufacturing porous structures for tissue engineering [8]. Processes of SL are integrated manufacturing processes, which include model slicing, laser devices control, materials, machine parameter setup, and post-processing modules [9]. SL process like the other AM technologies presents some imperfections in dealing with filling the space of the part without the generation of discontinuities. Such imperfections ranges from geometrical defects to volume mismatch. These defects impair the effectiveness of the AM process and in turn affect the performance of the designed parts. If the previously mentioned imperfections are genuine kinematics defects, another type is more specific to SL, namely inhomogeneous curing. This is the source for distortion and shrinkage phenomena that appear during the post-curing process. Dimension inaccuracy originates here from the uncured or partially cured resin within the photopolymer material [10]. Because of all mentioned imperfections, engineering

* Corresponding author. INRA, UR1268 Biopolymères Interactions Assemblages, F-44300 Nantes, France.
E-mail addresses: sofiane.guessasma@inra.fr (S. Guessasma), JH.Zhu_FEA@nwpu.edu.cn (J. Zhu), zhangwh@nwpu.edu.cn (W. Zhang).

https://doi.org/10.1016/j.eurpolymj.2017.10.034
Received 28 February 2017; Accepted 23 October 2017
Available online 28 October 2017

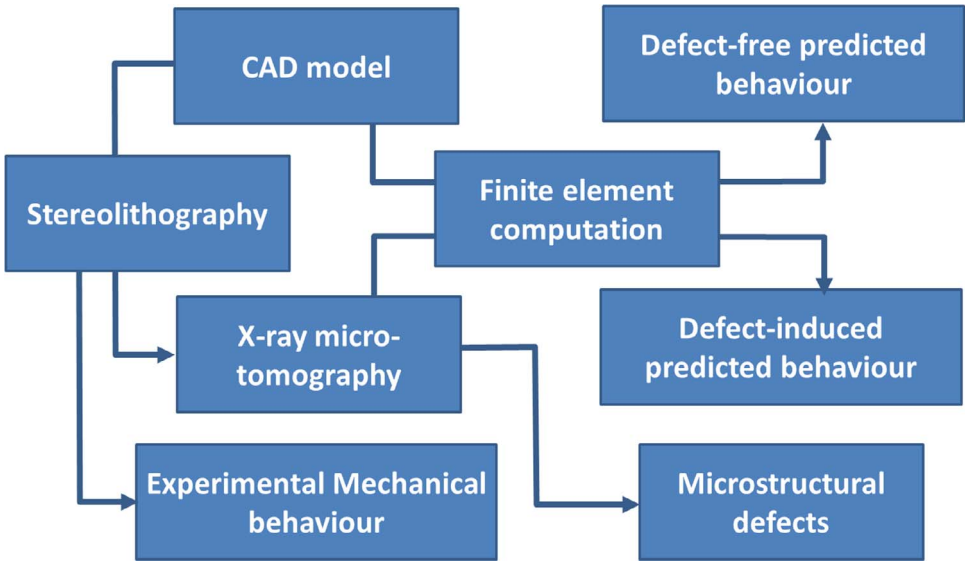

Fig. 1. General scheme of the approach used to derive the effect of process induced defects on mechanical performance of cellular parts with close porosities designed using stereolithography.

parameters received major attention for the purpose to optimise the process and improve the quality of the manufactured parts. In most situations arising, compromises are found. Slicing the CAD model prior printing is a typical example. Indeed, a small slice thickness leads to accurate geometry but large build time, while large slice thickness causes dimension errors and unsatisfying surface finish state due to staircasing. Several strategies have been developed to optimize the slicing procedure including direct slicing of CAD models with constant or adaptive layering thickness [11]. Physical parameters such as hatch cure depth, blade gap, hatch spacing and orientation have also being studied due to their large effect on the part quality. Zhou et al. [12] report five possible input process parameters that affect geometry accuracy with a leading influence of layer thickness and laser scanning duration. Chockalingam et al. [13] confirm the influential effect of layer thickness on mechanical properties of SL components more particularly residual stress and tensile strength. Build orientation as another process parameter directly affects the part accuracy, mechanical performance, build time and cost. Quintana et al. [14] demonstrate through a statistical design of experiments that the layout has a significant influence on tensile strength and stiffness. In fact, the layout influence is justified by the relative positioning of the layers composing the part with respect to the loading direction.

These flaws mentioned above are amplified when it comes to the design of cellular structures. The associated complex surface tessellation undermines the fabrication step more severely compared to dense structures. This problem is critical because of the large sensitivity of the in-service performance to cellular characteristics [15]. The amount of voids, for instance, tunes exponentially both strength and stiffness [16,17]. It appears then important to precisely quantify the influence of the complex porous architecture on the mechanical performance of SL-based parts. Analytical methods are often limited to predict such rendering of complex architectures, while numerical approaches like finite element (FE) method are more accurate especially to incorporate microstructural details [18]. This strategy of using FE based models is applied by Campoli et al. [19] to evaluate the mechanical performance of cellular structures manufactured using selective melting. To be even more effective, FE computations are to be coupled with adequate 3D imaging techniques to access microstructural defects. Veyhl et al. [20] point out the mechanical anisotropy of cellular structures that can be reached using FE models combined with micro-computed tomography.

As shown in Fig. 1, the sensing of the microstructural defect role on part performance is considered through a scheme involving 3D imaging, finite element computation and mechanical testing. The idea here is to compare the predicted behaviour of the cellular structures based on implementation, in the finite element model, of microstructural information issued from 3D imaging.

This defect based model is compared to predictions relying on CAD model geometries. The difference between the two predictions is informative of microstructural defect influence, which is precisely evaluated and quantified in this study. The comparison with the experimental testing result (Fig. 1) provides a key understanding of the role of defects in driving the performance of porous parts designed using stereolithography.

2. Experimental layout

2.1. Cellular structure processing

The cellular solids are designed using sequential addition algorithm based on random positioning of voids with typical diameter of nearly 10 mm each. The spherical porosities are allowed to overlap to increase the porous content from 0 up to 60%. In order to guarantee structural stability of the cellular material, void positioning is accepted at the condition of solid material continuity. The CAD models of typical dimensions of $(30 \times 30 \times 30)$ mm^3 are converted into stl files. The

Table 1
Photosensitive resin SPR6000B: Physical characteristics of the liquid and post-cured states.

Liquid state	
Appearance	White
Density	1.13 g/cm^3 at 25 °C
Viscosity	355 cps at 28 °C
Penetration distance, Dp	0.145 mm
Critical exposure energy, Ec	9.3 mJ/cm^2
Building layer thickness	0.1 mm

Post-cured solid state (90-min UV post-cure)		
Property	Test standard	Magnitude
Hardness, Shore D	ASTM D 2240	83
Flexural modulus	ASTM D 790	2692–2775 MPa
Flexural strength	ASTM D 790	69–74 MPa
Tensile modulus	ASTM D 638	2189–2395 MPa
Tensile strength	ASTM D 638	27–31 MPa
Elongation at break	ASTM D 638	12–20%
Impact strength	ASTM D 256 (notched Izod)	58–70 J/m
Heat deflection temperature	ASTM D 648 at 66 psi	52 °C
Glass transition (Tg)	DMA, E"peak	62 °C
Coefficient of thermal expansion	TMA (T < Tg)	97 × 10^{-6}/°C
Density	–	1.16 g/cm^3